CHALMERS

FINITE ELEMENT CENTER

PREPRINT 2002-11

Discontinuous/Continuous Least-Squares Finite Element Methods for Elliptic Problems

Rickard Bergström and Mats G. Larson

Chalmers Finite Element Center
CHALMERS UNIVERSITY OF TECHNOLOGY
Göteborg Sweden 2002

CHALMERS FINITE ELEMENT CENTER

Preprint 2002-11

Discontinuous/Continuous Least-Squares Finite Element Methods for Elliptic Problems

Rickard Bergström and Mats G. Larson

CHALMERS

Chalmers Finite Element Center
Chalmers University of Technology
SE–412 96 Göteborg Sweden
Göteborg, December 2002

Discontinuous/Continuous Least-Squares Finite Element Methods for Elliptic Problems
Rickard Bergström and Mats G. Larson
NO 2002-11
ISSN 1404–4382

Chalmers Finite Element Center
Chalmers University of Technology
SE–412 96 Göteborg
Sweden
Telephone: +46 (0)31 772 1000
Fax: +46 (0)31 772 3595
www.phi.chalmers.se

Printed in Sweden
Chalmers University of Technology
Göteborg, Sweden 2002

Discontinuous/Continuous Least-Squares Finite Element Methods for Elliptic Problems *

Rickard Bergström† and Mats G. Larson‡

Abstract

Least-squares finite element methods typically suffer from requirements on the solution to be very regular. This rules out, e.g., applications posed on nonconvex domains. In this paper we study a least-squares formulation where the discrete space is enriched by discontinuous elements in the vicinity of singularities, making computation of less regular problems possible. We apply this technique to the first order Poisson problem, show coercivity and a priori estimates, and present numerical results in 3D.

1 Introduction

Despite the fact that the least-squares finite element method (LSFEM) suffers from several short comings, mainly concerning the regularity of the exact solution, the advantages it offers, such as yielding symmetric positive definite matrix problems, have made the method attractive in several areas. Applications include among others the convection-diffusion equation [22], the Stokes [5] and the Navier-Stokes equations [4], Helmholtz' equation [21], Navier's equation [11], and Maxwell's equations [19]. For a review of the least-squares finite element method and more references to the mentioned applications, we refer to the paper by Bochev and Gunzberger [6].

This paper is concerned with the complication involving nonconvex polyhedral domains, possibly in the context of an interface problem. The difficulty that arises with the least-squares finite element method is due to the strong regularity requirement for the method, a requirement only fulfilled in smooth domains. In [14], weighted L^2-norms were used in two space dimensions to achieve optimal convergence. A similar formulation is studied in [20] for an interface problem. Also in [13], a weighted norm is used when stabilizing Maxwell's

*Research supported by ABB Corporate Research, Sweden

†Supported by the Swedish Foundation for Strategic Research through the National Graduate School in Scientific Computing and the National Network in Applied Mathematics

‡Supported by Swedish Research Council for Engineering Sciences

equations with a quadratic divergence term. This approach, however, requires a precise knowledge of the behaviour of the solution at the geometric singularity, a knowledge which one may not have.

Another approach is based on a discrete minus one inner product by Bramble *et al.* [7]. Combined with the Raviart-Thomas elements a formulation which is optimal with respect to regularity and approximation on general polygonal domains is derived. The construction of the inner product leads however to dense matrices.

Here we study a least-squares formulation, based on the use of discontinuous elements to approximate $H(\mathrm{div})$, which allows us to get optimal estimates in the $H(\mathrm{div})$-norm. The interface problem has been handled in [12] and we use a similar approach. The introduction of discontinuous elements in this setting was made by Bramble *et al.*[8].

We prove optimal convergence results for the method applied to the first order system formulation of the Poisson problem. Moreover, we present numerical results for model problems in three spatial dimensions. In order to reduce computational cost, we introduce an adaptive hybrid scheme based on discontinuous approximation only in the vicinity of singularities and continuous approximation elsewhere, combined with adaptive mesh refinement.

The model problems include a line singularity, a point singularity, and an interface problem including both types of singularities. The proposed hybrid scheme performs well for all these problems. In some cases, depending on the formulation of the boundary conditions, we find that also the standard least-squares method performs surprisingly well, but does not capture the singularity correctly.

The rest of this paper is organized as follows. In Section 2, we present the problem and formulate the discontinuous/continuous least-squares method; in Section 3, we state and prove coercivity of the bilinear form and a priori error estimates based on interpolation on the BDM spaces and introduce variations on the scheme; in Section 4, we introduce the adaptive hybrid formulation for efficient computations and discuss adaptivity issues; in Section 5, we present the numerical results.

2 The least-squares finite element method

2.1 Model problem

We consider the problem: find u such that

$$-\nabla \cdot A\nabla u = f \quad \text{in } \Omega, \tag{1a}$$

$$n \cdot A\nabla u = g_N \quad \text{on } \Gamma_N, \tag{1b}$$

$$u = g_D \quad \text{on } \Gamma_D, \tag{1c}$$

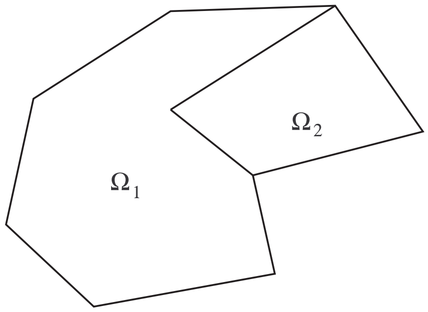

Figure 1: A polygonal domain with two subdomains.

where $\Omega \subset \mathbf{R}^3$ is a polyhedral domain with boundary $\Gamma = \Gamma_D \cup \Gamma_N$, see Grisvard [17] for a definition, $f \in L^2(\Omega)$, n is the exterior unit normal, $g_N \in H^{1/2}(\Gamma_N)$ and $g_D \in H^{3/2}(\Gamma_D)$. A is a symmetric piecewise constant matrix $A = A^i$ for $x \in \Omega^i$, with $\{\Omega^i\}$ a partition of Ω into polyhedral subdomains Ω^i. Further we assume that there are constants c_A and C_A such that $c_A|x|^2 \leq x \cdot Ax \leq C_A|x|^2$.

Introducing the flux

$$\sigma = A\nabla u, \tag{2}$$

we may write problem (1) as the first order system: find (u, σ) such that

$$-\nabla \cdot \sigma = f \quad \text{in } \Omega, \tag{3a}$$
$$\sigma - A\nabla u = 0 \quad \text{in } \Omega, \tag{3b}$$
$$n \cdot \sigma = g_N \quad \text{on } \Gamma_N, \tag{3c}$$
$$u = g_D \quad \text{on } \Gamma_D. \tag{3d}$$

Under our assumptions on data, the solution (u, σ) to (3) resides in at least $H^1(\Omega) \times H(\text{div}; \Omega)$, with u uniquely determined if $\Gamma_D \neq \emptyset$. To be more precise, we have for a nonconvex Ω, that the minimal regularity for u is $H^{3/2+\delta}(\Omega)$, with $0 < \delta < 1/2$ depending on the geometry, and consequently, for σ we have $[H^{1/2+\delta}(\Omega)]^3$, see e.g. [1], [15], and [17]. By minimal regularity, we mean that for some f, there are solutions u such that $u \notin H^{3/2+\delta}(\Omega)$, but $u \in H^{3/2+\delta-\epsilon}(\Omega)$, for all $\epsilon > 0$ [2]. We denote the space in which the solution resides by $\mathcal{V} \times \mathcal{W}$. The space $H(\text{div}; \Omega)$ mentioned above is defined as

$$H(\text{div}; \Omega) = \{v \in [L^2(\Omega)]^3 : \nabla \cdot v \in L^2(\Omega)\}, \tag{4}$$

and is a Sobolev space with the product norm

$$\|v\|^2_{H(\text{div})} = \|\nabla \cdot v\|^2 + \|v\|^2. \tag{5}$$

2.2 Finite element spaces

Let $\mathcal{K}$ be a triangulation of Ω into shape regular tetrahedra K which respects the subdomains, i.e., all $K \subset \Omega^i$ for some i. Denote the set of all faces F by $\mathcal{F}$ and divide it into three disjoint sets

$$\mathcal{F} = \mathcal{F}_I \cup \mathcal{F}_D \cup \mathcal{F}_N, \tag{6}$$

where $\mathcal{F}_I$ is the set of all faces in the interior of Ω, $\mathcal{F}_D$ the faces on the Dirichlet part of the boundary Γ_D, and $\mathcal{F}_N$ the faces on the Neumann part Γ_N. We let $h : \Omega \to \mathbf{R}$ denote the mesh function such that $h|_K = h_K = \mathrm{diam}(K)$ and $h|_F = h_F = \mathrm{diam}(F)$, i.e., a measure of the size of the element K or the face F. Finally, we define the piecewise polynomial space

$$\mathcal{V}_h \times \mathcal{W}_h = \mathcal{CP}_p \times [\mathcal{DP}_p]^3, \tag{7}$$

where

$$\mathcal{CP}_p = \mathcal{DP}_p \cap C(\Omega), \tag{8}$$

$$\mathcal{DP}_p = \bigoplus_{K\in\mathcal{K}} \mathcal{P}_p(K), \tag{9}$$

and $\mathcal{P}_p(K)$ is the space of all polynomials of degree less than or equal to p defined on K. The degree of the polynomials, as well as the meshsize, may vary from element to element so that $p|_K = p_K$, and thus we allow h-p adaptivity.

2.3 The discontinuous/continuous least-squares finite element method

The discontinuous/continuous least-squares finite element method (D/C LSFEM) reads: find $(u_h, \sigma_h) \in \mathcal{V}_h \times \mathcal{W}_h$ such that

$$I(u_h, \sigma_h) = \inf_{(v,\chi)\in\mathcal{V}_h\times\mathcal{W}_h} I(v, \chi), \tag{10}$$

where the least-squares functional $I(\cdot, \cdot)$ is defined by

$$\begin{aligned} I(v,\chi) = &\sum_{K\in\mathcal{K}} \left(\|\nabla\cdot\chi + f\|_K^2 + \|A^{-1/2}(\chi - A\nabla v)\|_K^2\right) \\ &+\sum_{F\in\mathcal{F}_I}\|h^{-1/2}[n\cdot\chi]\|_F^2 + \sum_{F\in\mathcal{F}_N}\|n\cdot(\chi - g_N)\|_F^2 + \sum_{F\in\mathcal{F}_D}\|h^{-1/2}(v - g_D)\|_F^2. \end{aligned} \tag{11}$$

Note that the both Dirichlet (3c) and Neumann (3d) boundary conditions as well as normal continuity of the flux on interior faces, are imposed weakly through the least-squares functional. Furthermore, we assume that boundary data can be represented by functions in the finite element space.

Remark 2.1 We have the option of applying a weighting of the different terms in the least-squares functional by inserting a constant in front of each term, and still get equivalent schemes [12][25]. For a clearer presentation we have not included these weights in the notation.

The corresponding variational equation takes the form: find $(u_h, \sigma_h) \in \mathcal{V}_h \times \mathcal{W}_h$ such that

$$a(u_h, \sigma_h; v, \chi) = l(v, \chi), \tag{12}$$

for all $(v, \chi) \in \mathcal{V}_h \times \mathcal{W}_h$. Here $a(\cdot\, ; \cdot)$ is a bilinear form and $l(\cdot)$ a linear functional, defined by

$$\begin{aligned} a(u, \sigma; v, \chi) = & \sum_{K \in \mathcal{K}} (\nabla \cdot \sigma, \nabla \cdot \chi)_K + (A^{-1}(\sigma - A\nabla u), (\chi - A\nabla v))_K \\ & + \sum_{F \in \mathcal{F}_I} (h^{-1}[n \cdot \sigma], [n \cdot \chi])_F \\ & + \sum_{F \in \mathcal{F}_N} (n \cdot \sigma, n \cdot \chi)_F \\ & + \sum_{F \in \mathcal{F}_D} (h^{-1} u, v)_F \end{aligned} \tag{13a}$$

$$l(v, \chi) = \sum_{K \in \mathcal{K}} (f, \nabla \cdot \chi)_K + \sum_{F \in \mathcal{F}_N} (g_N, n \cdot \chi)_F + \sum_{F \in \mathcal{F}_D} (h^{-1} g_D, v)_F. \tag{13b}$$

3 Error estimates

3.1 Coercivity and continuity

We begin our analysis by introducing the (semi) norm

$$\begin{aligned} |||(u, \sigma)|||^2 = & \sum_{K \in \mathcal{K}} \left(\|\nabla \cdot \sigma\|_K^2 + \|A^{-1/2}\sigma\|_K^2 + \|A^{1/2}\nabla u\|_K^2 \right) \\ & + \sum_{F \in \mathcal{F}_I} \|h^{-1/2}[n \cdot \sigma]\|_F^2 + \sum_{F \in \mathcal{F}_N} \|n \cdot \sigma\|_F^2 + \sum_{F \in \mathcal{F}_D} \|h^{-1/2} u\|_F^2. \end{aligned} \tag{14}$$

We then have the following basic estimates.

Proposition 3.1 *It holds*

$$m|||(u, \sigma)|||^2 \leq a(u, \sigma; u, \sigma) \qquad \forall (u, \sigma) \in \mathcal{V}_h \times \mathcal{W}_h, \tag{15}$$

$$a(u, \sigma; v, \chi) \leq M|||(u, \sigma)|||\, |||(v, \chi)||| \quad \forall (u, \sigma) \text{ and } (v, \chi) \in \mathcal{V} \times \mathcal{W}, \tag{16}$$

with constants m and M independent of h.

Remark 3.1 In our analysis, we do not consider m and M's dependence on A. Following [20] it is reasonable to believe that these constant do not depend on the size of the discontinuities of A, only its variations in each subdomain.

In order to prove Proposition 3.1, we need the following version of Poincare's inequality.

Lemma 3.2 *For $v \in H^1(\Omega)$, we have*

$$\|v\|_\Omega^2 \leq C \left(\|\nabla v\|_\Omega^2 + \|v\|_{\Gamma_D}^2 \right). \tag{17}$$

Proof of Proposition 3.1. To prove (15) we start from the definition (13a) of the bilinear form

$$\begin{aligned} a(u,\sigma;u,\sigma) = &\sum_{K\in\mathcal{K}} \left(\|\nabla\cdot\sigma\|_K^2 + \|A^{-1/2}(\sigma - A\nabla u)\|_K^2 \right) \\ &+ \sum_{F\in\mathcal{F}_I} \|h^{-1/2}[n\cdot\sigma]\|_F^2 + \sum_{F\in\mathcal{F}_N} \|n\cdot\sigma\|_F^2 + \sum_{F\in\mathcal{F}_D} \|h^{-1/2}u\|_F^2. \end{aligned} \tag{18}$$

We have

$$\|A^{-1/2}\sigma - A^{1/2}\nabla u\|^2 = \|A^{-1/2}\sigma\|^2 - (\nabla u,\sigma) + \|A^{1/2}\nabla u\|^2 \tag{19}$$

$$\geq \|A^{-1/2}\sigma\|^2 - |(\nabla u,\sigma)| + \|A^{1/2}\nabla u\|^2. \tag{20}$$

We thus only need to estimate $|(\nabla u,\sigma)|$. Using Green's formula we get

$$(\nabla u,\sigma) = -\sum_{K\in\mathcal{K}} (u,\nabla\cdot\sigma)_K + \sum_{F\in\mathcal{F}_I} (u,[n\cdot\sigma])_F + \sum_{F\in\mathcal{F}_N\cup\mathcal{F}_D} (u,n\cdot\sigma)_F. \tag{21}$$

The first term on the right hand side in (21) may be estimated using the Cauchy-Schwarz and ϵ-inequalities followed by an application of Lemma 3.2,

$$\begin{aligned} \sum_{K\in\mathcal{K}} (u,\nabla\cdot\sigma)_K &\leq C\epsilon\|u\|^2 + C\epsilon^{-1}\|\nabla\cdot\sigma\|^2 \\ &\leq C\epsilon \left(\|A^{1/2}\nabla u\|^2 + \sum_{F\in\mathcal{F}_D} \|h^{-1/2}u\|_F^2 \right) + C\epsilon^{-1}\|\nabla\cdot\sigma\|^2, \end{aligned} \tag{22}$$

for any $\epsilon > 0$ and $h \leq 1$. Next, for the second term, we again invoke the Cauchy-Schwarz and ϵ-inequalities to get

$$\sum_{F\in\mathcal{F}_I} (u,[n\cdot\sigma])_F \leq C \sum_{F\in\mathcal{F}_I} \epsilon\|h^{1/2}u\|_F^2 + \epsilon^{-1}\|h^{-1/2}[n\cdot\sigma]\|_F^2 \tag{23}$$

$$\leq C\epsilon \left(\sum_{K\in\mathcal{K}} \|A^{1/2}\nabla u\|_K^2 + \sum_{F\in\mathcal{F}_D} \|h^{-1/2}u\|_F^2 \right) \tag{24}$$

$$+ C\epsilon^{-1} \sum_{F\in\mathcal{F}_I} \|h^{-1/2}[n\cdot\sigma]\|_F^2. \tag{25}$$

Here we estimated the first term on the right hand side in (23) using elementwise trace inequalities followed by Lemma 3.2,

$$\sum_{F\in\mathcal{F}_I} \|h^{1/2}u\|_F^2 \leq C \sum_{K\in\mathcal{K}} \|u\|_K^2 + h^2\|\nabla u\|_K^2 \tag{26}$$

$$\leq C \left(\sum_{K\in\mathcal{K}} \|A^{1/2}\nabla u\|_K^2 + \sum_{F\in\mathcal{F}_D} \|h^{-1/2}u\|_F^2 \right). \tag{27}$$

Finally, the third term on the right hand side in (21) can with the same technique be estimated as follows:

$$\sum_{F\in\mathcal{F}_D\cup\mathcal{F}_N}(u,n\cdot\sigma)_F \leq C\sum_{F\in\mathcal{F}_D}\left(\epsilon^{-1}\|h^{-1/2}u\|_F^2+\epsilon\|h^{1/2}n\cdot\sigma\|_F^2\right) \tag{28}$$

$$+C\sum_{F\in\mathcal{F}_N}\left(\epsilon\|u\|_F^2+\epsilon^{-1}\|n\cdot\sigma\|_F^2\right)$$

$$\leq C\epsilon\sum_{K\in\mathcal{K}}\left(\|A^{1/2}\nabla u\|_K^2+\|A^{-1/2}\sigma\|_K^2\right) \tag{29}$$

$$+C\epsilon^{-1}\sum_{F\in\mathcal{F}_N}\|n\cdot\sigma\|_F^2+C(\epsilon+\epsilon^{-1})\sum_{F\in\mathcal{F}_D}\|h^{-1/2}u\|_F^2,$$

for all $\epsilon>0$. In (29) we used the inverse inequality

$$\|h^{1/2}n\cdot\sigma\|_{\partial K}\leq C\|A^{-1/2}\sigma\|_K, \tag{30}$$

for $\sigma\in\mathcal{P}_p(K)$. Note that the constant C depends on the order of polynomials p. Collecting these estimates, we get

$$|(\nabla u,\sigma)|\leq C_1\epsilon\sum_{K\in\mathcal{K}}\left(\|A^{1/2}\nabla u\|_K^2+\|A^{-1/2}\sigma\|_K^2\right)+C_2\epsilon^{-1}\sum_{K\in\mathcal{K}}\|\nabla\cdot\sigma\|_K^2$$

$$+C_2\epsilon^{-1}\left(\sum_{F\in\mathcal{F}_N}\|n\cdot\sigma\|_F^2+\sum_{F\in\mathcal{F}_I}\|h^{-1/2}[n\cdot\sigma]\|_F^2\right) \tag{31}$$

$$+(C_1\epsilon+C_2\epsilon^{-1})\sum_{F\in\mathcal{F}_D}\|h^{-1/2}u\|_F^2.$$

Inserting (31) into (18) and (19), we get

$$a(u,\sigma;u,\sigma)\geq(1-C_2\epsilon^{-1})\sum_{K\in\mathcal{K}}\|\nabla\cdot\sigma\|_K^2 \tag{32}$$

$$+(1-C_1\epsilon)\sum_{K\in\mathcal{K}}\left(\|A^{-1/2}\sigma\|_K^2+\|A^{1/2}\nabla u\|_K^2\right)$$

$$+(1-C_2\epsilon^{-1})\left(\sum_{F\in\mathcal{F}_N}\|n\cdot\sigma\|_F^2+\sum_{F\in\mathcal{F}_I}\|h^{-1/2}[n\cdot\sigma]\|_F^2\right)$$

$$+(1-C_1\epsilon-C_2\epsilon^{-1})\sum_{F\in\mathcal{F}_D}\|h^{-1/2}u\|_F^2.$$

Choosing ϵ such that $C_1\epsilon\leq 1/2$ and increasing the weights α_i on the remaining terms so that $\alpha_i-C_2\epsilon^{-1}>0$, we have

$$\tilde{a}(u,\sigma;u,\sigma)\geq m|||(u,\sigma)|||^2, \tag{33}$$

where $\tilde{a}(\cdot,\cdot)$ denotes the weighted least-squares functional, see Remark 2.3. Finally, we note that all forms with positive weights are equivalent and thus the proof of (15) follows.

The continuity (16) is a direct consequence of the Cauchy-Schwarz and triangle inequalities. □

3.2 A priori error estimates

We begin by introducing the interpolation operator, $\Pi : (u,\sigma) \mapsto (\pi_u u, \pi_\sigma \sigma)$, with π_u the standard Scott-Zhang interpolation operator, see [23], and π_σ an interpolation operator onto the Brezzi-Douglas-Marini (BDM) spaces, see [10]. These elements have the degrees of freedom associated with the moments of the field in the interior of the element and the normal trace on the faces. The BDM-interpolant ensures normal continuity across element faces and can be defined for functions satisfying $\sigma \in [L^s]^3$ and $\nabla\cdot\sigma \in L^2$, with $s > 2$. This restriction is necessary to define the normal traces of the definition and we remark that solutions to (1) satisfy this condition. The most important property of π_σ is that on an affine element,

$$\nabla \cdot \pi_\sigma \sigma = P_{p-1,K} \nabla \cdot \sigma, \tag{34}$$

where $P_{p-1,K}$ denotes the $L^2(K)$-projection onto $\mathcal{P}_{p-1}(K)$. This identity can be seen by elementwise integration by parts and using the definition of the interpolant, see [9].

We then have the following interpolation error estimate.

Lemma 3.3 *Let K be an affine element and π_σ the BDM-interpolation operator. Then there is a constant C depending only on the polynomial order and the shape of K, such that*

$$\|(\sigma - \pi_\sigma\sigma)\|_K \leq C h_K^\alpha |\sigma|_{\alpha,K}, \qquad 1/2 < \alpha \leq p+1, \tag{35a}$$
$$\|\nabla\cdot(\sigma - \pi_\sigma\sigma)\|_K \leq C h_K^\alpha |\nabla\cdot\sigma|_{\alpha,K}, \qquad 0 < \alpha \leq p. \tag{35b}$$

An estimate in the energy norm can now be formulated.

Lemma 3.4 *For $(u,\sigma) \in H^{s+1}(\Omega) \times H^s(div;\Omega)$, with $s > 0$, it holds*

$$|||(u,\sigma) - (\pi_u u, \pi_\sigma \sigma)|||^2 \leq C \sum_{K\in\mathcal{K}} h_K^{2\alpha} \big(\|\nabla\cdot\sigma\|_{\alpha,K}^2 + \|\sigma\|_{\alpha,K}^2 + \|u\|_{\alpha+1,K}^2 \big), \tag{36}$$

with $\alpha = \min(p,s)$.

Proof. Note that the BDM-interpolant of σ has continuous normal component, so all interior face terms cancel. The boundary conditions may be exactly represented in the approximating space and are thus also zero. The result then follows by applying Lemma 3.3 and the corresponding estimate for the Scott-Zhang interpolator [23]. □

Now, we are ready to state the following main result:

Theorem 3.5 *Let* $(u, \sigma) \in H^{s+1}(\Omega) \times H^s(div;\Omega)$ *with* $s > 0$ *be the exact solution to (3) and* $(u_h, \sigma_h) \in \mathcal{V}_h \times \mathcal{W}_h$ *the approximate solution defined by (12). Then it holds*

$$|||(u - u_h, \sigma - \sigma_h)|||^2 \leq C \sum_{K\in\mathcal{K}} h_K^{2\alpha} \big(\|\nabla \cdot \sigma\|^2_{\alpha,K} + \|\sigma\|^2_{\alpha,K} + \|u\|^2_{\alpha+1,K}\big), \tag{37}$$

with $\alpha = \min(p, s)$ *and the constant* C *independent of the meshsize* h.

Proof. We first add and subtract an interpolant and then use the triangle inequality to get

$$|||(u - u_h, \sigma - \sigma_h)||| \leq |||(u - \pi_u u, \sigma - \pi_\sigma\sigma)||| + |||(\pi_u u - u_h, \pi_\sigma\sigma - \sigma_h)|||. \tag{38}$$

For the second term, invoking coercivity (15), we obtain

$$\begin{aligned}
m|||(\pi_u u - u_h, &\pi_\sigma\sigma - \sigma_h)|||^2 && (39)\\
&\leq a\big((\pi_u u - u_h, \pi_\sigma\sigma - \sigma_h), (\pi_u u - u_h, \pi_\sigma\sigma - \sigma_h)\big) \\
&= a\big((\pi_u u - u, \pi_\sigma\sigma - \sigma), (\pi_u u - u_h, \pi_\sigma\sigma - \sigma_h)\big) && (40)\\
&\leq |||(\pi_u u - u, \pi_\sigma\sigma - \sigma)|||\;|||(\pi_u u - u_h, \pi_\sigma\sigma - \sigma_h)|||, && (41)
\end{aligned}$$

where we used the Galerkin orthogonality (12) in (40) and continuity of the bilinear form (16) in (41). Dividing by $|||(\pi_u u - u_h, \pi_\sigma\sigma - \sigma_h)|||$ and inserting this estimate in (38), we arrive at

$$\begin{aligned}
|||(u - u_h, \sigma - \sigma_h)|||^2 &\leq (1 + 1/m)^2|||(u - \pi_u u, \sigma - \pi_\sigma\sigma)|||^2 && (42)\\
&\leq C \sum_{K\in\mathcal{K}} h_K^{2\alpha} \big(\|\nabla \cdot \sigma\|^2_{\alpha,K} + \|\sigma\|^2_{\alpha,K} + \|u\|^2_{\alpha+1,K}\big),
\end{aligned}$$

where Lemma 3.4 was used in the last inequality. □

3.3 Variations on the same theme

Up to now, we have presented the method using nodal finite elements and only made the flux discontinuous. There are of course other ways to implement this formulation, which only leads to small variations in the analysis.

3.3.1 Discontinuous least-squares finite element method

For practical reasons, one may choose to have also u discontinuous. This will lead to easier implementation since we may group the unknowns into small blocks, one for each node. We would then add the term

$$\sum_{F\in\mathcal{F}_I} \|h^{-1/2}[u]\|^2 \tag{43}$$

to the least-squares functional (11) in order to impose continuity of u.

3.3.2 BDM/continuous least-squares finite element method

Instead of making the flux discontinuous and imposing the normal continuity weakly, one may instead use a conforming approximation of $H(\mathrm{div})$, such as the BDM or RT-elements [10]. As discussed in Section 3.2, this ensures continuity of $n \cdot \sigma$ at the interfaces and thus these terms will be zero in the least-squares functional.

4 An adaptive hybrid method

Since the solution to problem (3) is of low regularity only close to corners and edges and standard continuous finite elements work well to approximate the regular part of the solution, it is natural to combine completely continuous and discontinuous/continuous approximations. It is thus sufficient to use the discontinuous approximation in the vicinity of a geometric singularity, where the extra degrees of freedom inflicted by the discontinuous method pay off.

Denote by Ω_D a region, conforming with the triangulation $\mathcal{K}$, surrounding the geometric singularities, where we have to use D/C LSFEM, and let $\Omega_C = \Omega \backslash \Omega_D$. In Ω_C we have the solution $(u, \sigma) \in H^{s_C+1} \times [H^{s_C}]^3$, with $s_C \geq 1$, and may use continuous LSFEM with polynomials of degree p_C. If the decomposition $\Omega = \Omega_C \cup \Omega_D$ is chosen such that s_C is considerably larger than s, we can also benefit from this by using high order polynomials in Ω_C. Further, let $\mathcal{K}_D = \{K \in \mathcal{K} : K \subset \Omega_D \text{ or } \overline{K} \cap \overline{\Omega}_D \neq \emptyset\}$ be the elements covering Ω_D and the neighboring elements, and define $\mathcal{K}_C$ analogously.

We then have the following extension of our earlier a priori error estimate:

Theorem 4.1 *Let $(u, \sigma) \in H^{s+1}(\Omega) \times H^s(div; \Omega)$ with $s > 0$ be the exact solution to (3) and $(u_h, \sigma_h) \in \mathcal{V}_h \times \mathcal{W}_h$ the approximate solution of the hybrid method proposed in this section. Using the notation introduced above, it holds*

$$\begin{aligned} |||(u - u_h, \sigma - \sigma_h)|||^2 \leq C &\sum_{K \in \mathcal{K}_D} h_K^{2\alpha} \big(\|\nabla \cdot \sigma\|^2_{\alpha,K} + \|\sigma\|^2_{\alpha,K} + \|u\|^2_{\alpha+1,K} \big) \\ &+ C \sum_{K \in \mathcal{K}_C} h_K^{2\alpha_C} \big(\|\sigma\|^2_{\alpha_C+1,K} + \|u\|^2_{\alpha_C+1,K} \big), \end{aligned} \tag{44}$$

with $\alpha = \min(p, s)$ and $\alpha_C = \min(p_C, s_C)$ and the constant C independent of the meshsize.

The natural mesh refinement indicator in a least-squares method is the the functional we try to minimize, i.e.,

$$\begin{aligned} \eta_K = &\|\nabla \cdot \sigma + f\|^2_K + \|A^{-1/2}(\sigma - A\nabla u)\|^2_K \\ &+ \|h^{-1/2}[n \cdot \sigma]\|^2_{\partial K \cap \mathcal{F}_I} + \|n \cdot (\sigma - g_N)\|^2_{\partial K \cap \mathcal{F}_N} \\ &+ \|h^{-1/2}(u - g_D)\|^2_{\partial K \cap \mathcal{F}_D}, \end{aligned} \tag{45}$$

where η_K denotes the element indicator. We use isotropic mesh refinement, splitting each element marked for refinement into two to eight new elements by successively dividing the

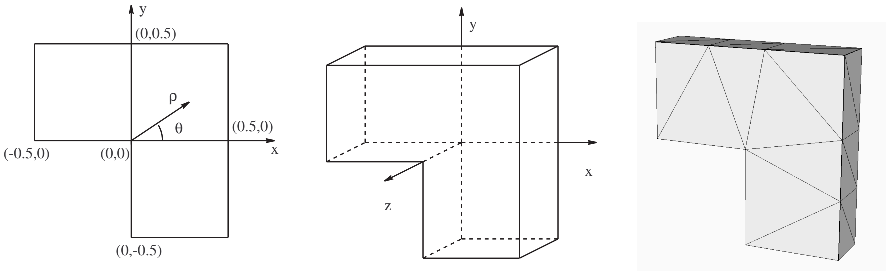

(a) *The x-y plane* (b) *The domain* (c) *Initial mesh*

Figure 2: The L-shaped domain with a line singularity.

longest edge, see [3] for more details. However, for problems with singularities like we treat in this paper, it would be desirable to use anisotropic or graded mesh refinement [16][24]. This seem to be an unexploited area in the least-squares society.

5 Numerical examples

In order to illustrate the theoretical results, we present numerical results for three examples, all computed in three spatial dimensions and using the adaptive method described in section 4: an L-shaped domain representing a line singularity, a sphere where a cone has been removed representing a point singularity, and finally a cube, where one octant has a different material parameter. For the first two examples analytic solutions are known.

5.1 Line singularity

We consider the problem

$$-\nabla \cdot \sigma = 0 \qquad \text{in } \Omega, \tag{46a}$$

$$\sigma - \nabla u = 0 \qquad \text{in } \Omega, \tag{46b}$$

$$u = g(\rho, \theta, z) \quad \text{on } \Gamma_D, \tag{46c}$$

$$n \cdot \sigma = 0 \qquad \text{on } \Gamma_N, \tag{46d}$$

where Ω is the domain showed in Figure 2 with $z \in (0, 0.2)$, $\Gamma_N = \{x \in \Omega; z = 0.0 \text{ or } z = 0.2\}$ and $\Gamma_D = \partial\Omega \backslash \Gamma_N$. The function g is chosen so that the exact solution of u is

$$u(\rho, \theta, z) = \rho^{2/3} \sin(2\theta/3 + \pi/3). \tag{47}$$

We remark that the solution is independent of the z-coordinate and is thus two dimensional.

The error for the discontinuous/continuous least-squares finite element method compared with standard LSFEM is presented in Figure 3. We clearly see that D/C LSFEM

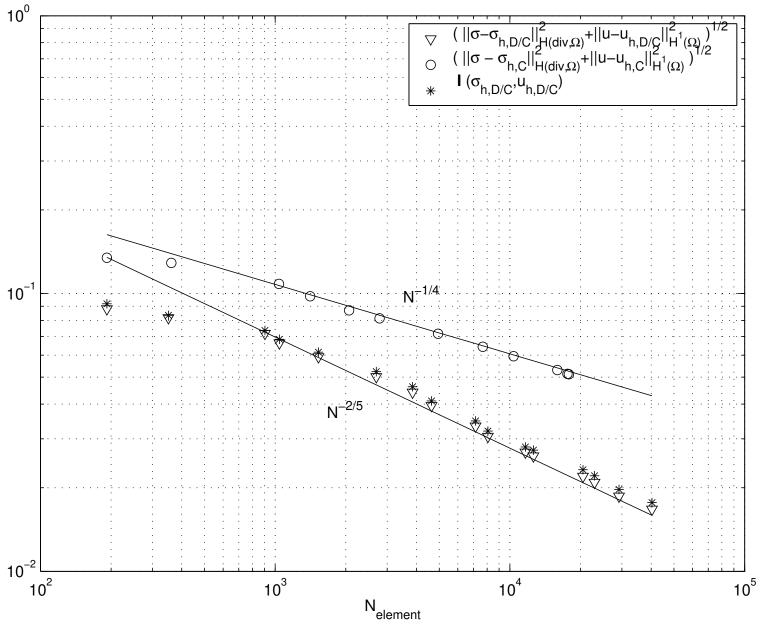

Figure 3: Error for standard LSFEM and D/C LSFEM in the line singularity example. Circles denote the error for standard LSFEM and triangles the error for D/C LSFEM measured in the $H^1(\Omega) \times H(\text{div};\Omega)$-norm; stars denote the D/C LSFEM residual.

shows better performance. The continuous method can not represent the solution correctly in the vicinity of the corner. It seems as if the geometry is rounded off and the singularity is absent. In Figure 4(a) we see that the computed flux is incorrect for standard LSFEM while, with discontinuous elements we can represent the solution correctly at the corner as in Figure 4(b). The error is however local and does not pollute the solution far from the singularity. We remark that the reason the standard LSFEM gives a solution that is only locally erroneous, is that on a Dirichlet boundary, and specifically in the corner, we have no condition on the flux σ . Thus the least-squares method is able to adapt in the way shown in Figure 4(a).

5.2 Point singularity

In this section we solve the following problem, described in spherical coordinates,

$$-\nabla \cdot \sigma = 0 \quad \text{in } \Omega, \tag{48a}$$

$$\sigma - \nabla u = 0 \quad \text{in } \Omega, \tag{48b}$$

$$u = P_\nu(\cos(\theta)) \quad \text{on } \Gamma_D, \tag{48c}$$

where $\Omega = \{(r, \theta, \phi) : r \in [0, 1), \theta \in (\beta, \pi], \phi \in [0, 2\pi)\}$ with $\beta = \pi/16$, P_ν is the first class Legendre function of order ν, and $\Gamma_D = \partial\Omega$. The exact solution of u to this problem is

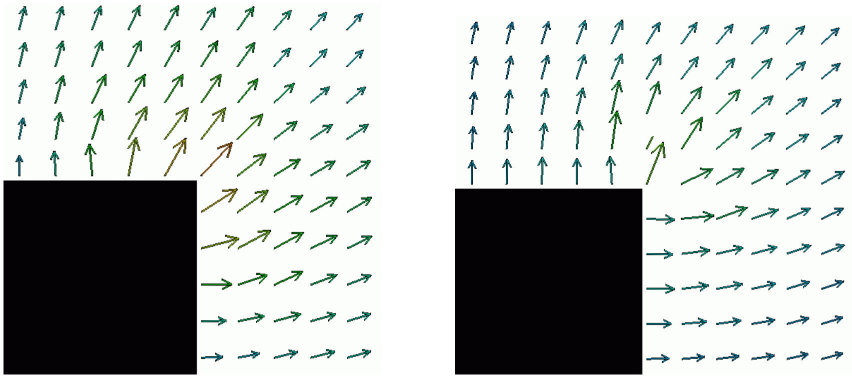

(a) *Standard LSFEM* (b) *D/C LSFEM*

Figure 4: The flux in the vicinity of the corner of the L-shaped domain. Note that for standard LSFEM, the flux is not correctly represented.

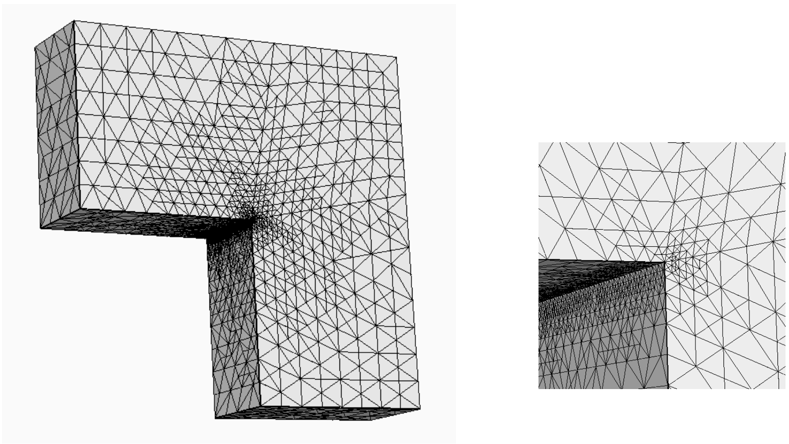

Figure 5: The mesh achieved after 20 refinement steps.

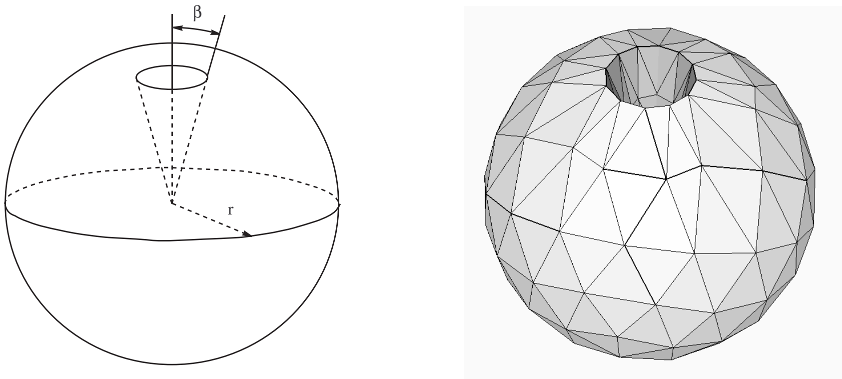

(a) *Geometry* (b) *Initial mesh*

Figure 6: The cone problem with a point singularity.

$$u(r, \theta) = r^{\nu} P_{\nu}(\cos(\theta)), \tag{49}$$

with ν depending on β; in our case $\nu \simeq 0.215$ for $\beta = \pi/16$, see [18].

Also in this problem, the Discontinuous/Continuous LSFEM is superior to the standard LSFEM, cf. Figure 7. The behaviour of the standard LSFEM is similar to the previous case and also here the singularity is absent.

5.3 Interface problem

In the previous examples, the material parameter is constant in the whole domain. We will now demonstrate an example where A has a jump across an interior interface. The domain is $\Omega = \Omega_1 \cup \Omega_2$ where $\Omega_1 = \{x \in (0, 0.5)^3\}$ and $\Omega_2 = \{x \in (0,1)^3\} \backslash \overline{\Omega}_1$.

The problem we solve is

$$-\nabla \cdot \sigma = 1 \quad \text{in } \Omega, \tag{50a}$$

$$\sigma - A\nabla u = 0 \quad \text{in } \Omega, \tag{50b}$$

$$u = 0 \quad \text{on } \Gamma_D. \tag{50c}$$

We choose $A_2 = 1.0$ and let $A_1 = \{10, 100, 1000\}$ for three different cases respectively. Figure 9(a) shows the domain and the initial mesh.

For this problem we do not have an exact solution to compare with. However, based on the experience of previous two examples, we rely on the least-squares functional as an error indicator.

Two methods were tested: first with continuous elements in each of the subdomains, but with weakly enforced interface conditions, and secondly with a layer of discontinuous elements around the interface.

The method with continuous elements in each subdomain shows a performance similar to the first example. Since the normal continuity is enforced only weakly, the standard

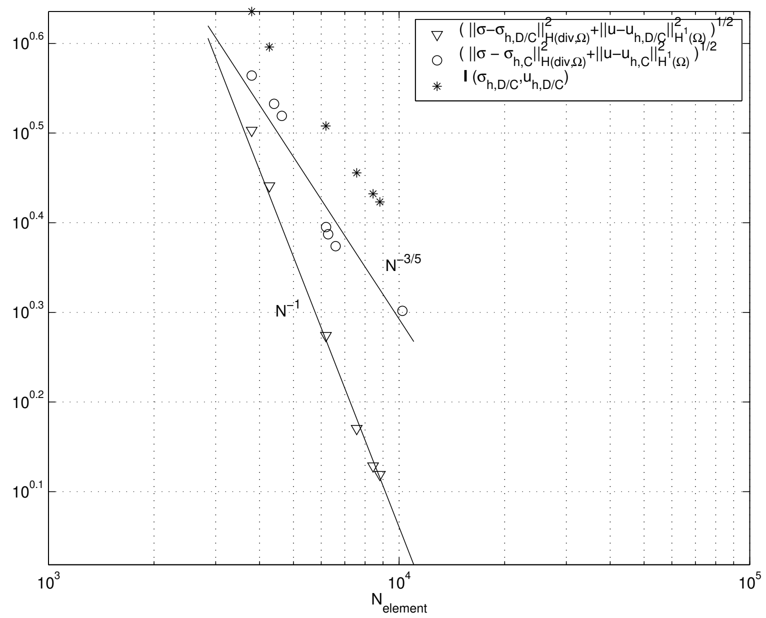

Figure 7: Error for standard LSFEM and D/C LSFEM in the cone singularity example. Circles denote the error for standard LSFEM and triangles the error for D/C LSFEM measured in the $H^1(\Omega) \times H(\text{div})(\Omega)$-norm; stars denote the D/C LSFEM residual.

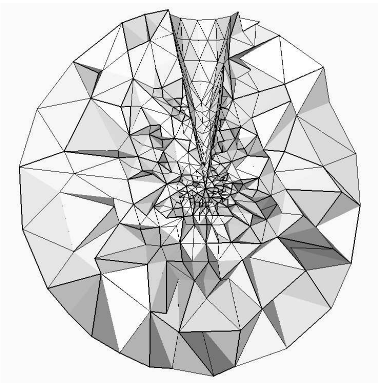

(a) *A slice through the mesh*

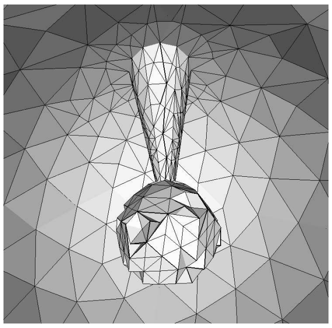

(b) *The ball with discontinuous elements at the cone tip*

Figure 8: The mesh achieved after 8 refinement steps.

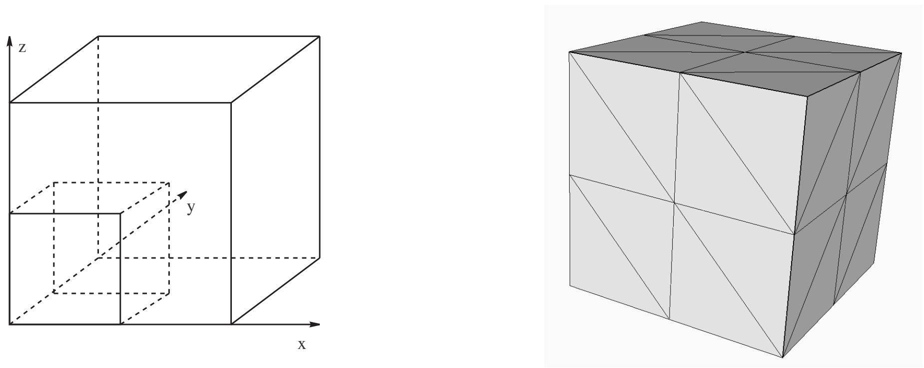

(a) *Geometry* (b) *Initial mesh*

Figure 9: The cube domain in the interface problem.

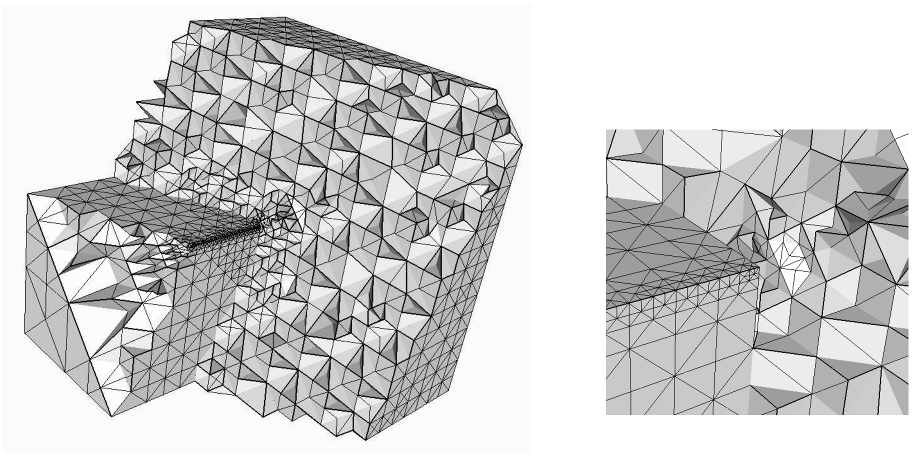

(a) *A slice through the mesh* (b) *Detail of the corner*

Figure 10: The mesh achieved after 14 refinement steps.

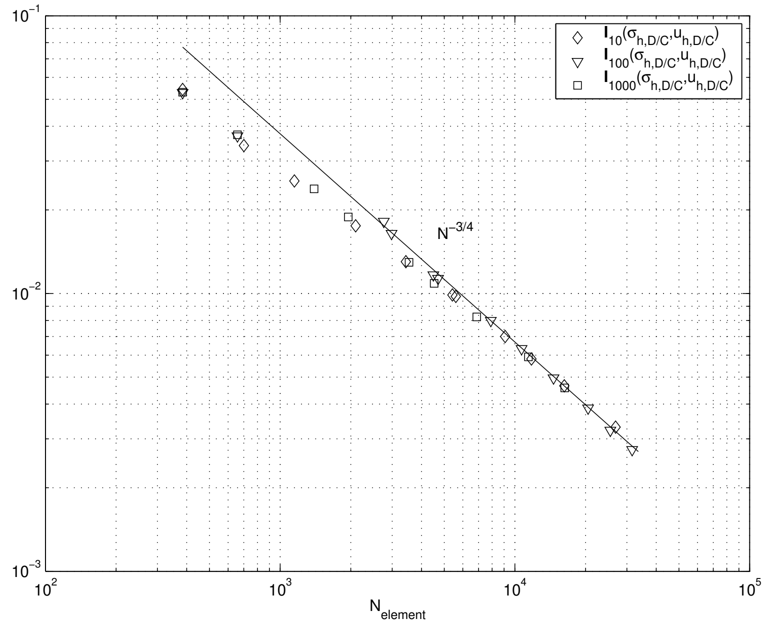

Figure 11: The least-squares functional for $A_1/A_2 = 10$ (diamonds), $A_1/A_2 = 100$ (triangles), and $A_1/A_2 = 1000$ (squares).

method is able to adapt by rounding off the corner as discussed in Section 5.1. We have therefore chosen not the present the convergence results for this setting.

The least-squares residual for the discontinuous/continuous solution in the three cases with different material parameters is shown in Figure 11. As we clearly see from the plot, the convergence is not affected by the ratio of the size of the parameters. However, with increasing ratio, the algebraic system of equations becomes more difficult to solve.

6 Conclusions

We have formulated and analysed the discontinuous/continuous least-squares finite element method. To obtain an efficient scheme, we propose an adaptive hybrid method based on discontinuous/continuous approximation only in the vicinity of singularities and fully continuous approximation elsewhere, combined with adaptive mesh refinement.

Furthermore, we present numerical results for the Poisson problem posed on nonconvex domains in three spatial dimensions, which lead to geometrical singularities in the solution, as well as an interface problem.

From the numerics, we see that the standard least-squares finite element method manages to produce a solution only as long as the conflicting conditions on the flux that causes the singularities, are not explicit in the problem. However, the computed solution does not capture the singularities and it appears the corners have been rounded off. This defect does not seem to pollute the solution.

In contrast, the proposed hybrid method performs well in all these cases, and the approximate solution displays a correct normal flux at the corner.

References

[1] C. Amrouche, C. Bernardi, M. Dauge, and V. Girault. Vector potentials in three-dimensional nonsmooth domains. *Math. Methods Appl. Sci.*, 21:823–864, 1998.

[2] F. Assous, P. Ciarlet, Jr., S. Labruine, and S. Lohrengel. The singular complement method. Unpublished.

[3] R. Bergström, M.G. Larson, and K. Samuelsson. The $\mathcal{L}\mathcal{L}^*$ finite element method and multigrid for the magnetostatic problem. Preprint 2, Chalmers Finite Element Center, Chalmers University of Technology, 2001.

[4] P. Bochev. Analysis of least-squares finite element methods for the Navier-Stokes equations. *SIAM J. Numer. Anal.*, 34:1817–1844, 1997.

[5] P. Bochev and M. Gunzburger. Analysis of least-squares finite element methods for for the Stokes equations. *Math. Comp.*, 63:479–506, 1994.

[6] P.B. Bochev and M.D. Gunzburger. Finite element methods of least-squares type. *SIAM Rev.*, 40(4):789–837, 1998.

[7] J.H. Bramble, R.D. Lazarov, and J.E. Pasciak. A least-squares approach based on a discrete minus one inner product for first order systems. *Math. Comp.*, 66(219):935–955, 1997.

[8] J.H. Bramble, R.D. Lazarov, and J.E. Pasciak. Least-squares for second order elliptic problems. *Comput. Methods in Appl. Mech. Engrg.*, 152:195–210, 1998.

[9] S.C. Brenner and L.R. Scott. *The Mathematical Theory of Finite Element Methods.* Springer-Verlag, 1994.

[10] F. Brezzi and M. Fortin. *Mixed and Hybrid Finite Element Methods.* Springer-Verlag, 1991.

[11] Z. Cai, T.A. Mantueffel, S.F. McCormick, and S. Parter. First-order system least squares for planar linear elasticity: pure traction. *SIAM J. Numer. Anal.*, (35):320–335, 1998.

[12] Y. Cao and M.D. Gunzberger. Least-squares finite element approximations to solutions of interface problems. *SIAM J. Numer. Anal.*, 35(1):393–405, 1998.

[13] M. Costabel and M. Dauge. Weigthed regularization of Maxwell equations in polyhedral domains. Unpublished.

[14] C.L. Cox and G.J. Fix. On the accuaracy of least squares methods in the presence of corner singularities. *Comp. & Maths. with Appls.*, 10(6):463–475, 1984.

[15] M. Dauge. *Elliptic Boundary Value Problems on Corner Domains.* Lecture Notes in Mathematics. Springer-Verlag, 1980.

[16] L. Formaggia and S. Perotto. Anisotropic error estimates for elliptic problems. Technical Report 18.2000, Dept. of Mathematics, Lausanne, 2000.

[17] P. Grisvard. *Elliptic Problems in Nonsmooth Domains.* Pitman Publishing Inc., 1985.

[18] J.D. Jackson. *Classical Electrodynamics.* John Wiley & Sons, 2nd edition, 1975.

[19] B.-N. Jiang, J. Wu, and L.A. Povinelli. The origin of spurious solutions in computational electromagnetics. *J. Comp. Phys.*, 125:104–123, 1996.

[20] T.A. Manteuffel, S.F. McCormick, and G. Starke. First-order system of least-squares for second order elliptic problems with discontinuous coefficients. To appear.

[21] P. Monk and D.-Q. Wang. A least-squares method for the Helmholtz equation. *Comput. Metods Appl. Mech. Engrg.*, 175:121–136, 1999.

[22] A.I. Pehlivanov, G.F. Carey, and P.S. Vassilevski. Least-squares mixed finite element methods for non-selfadjoint problems: I. error estimates. *Numer. Math.*, 72:501–522, 1996.

[23] L.R. Scott and S. Zhang. Finite element interpolation of nonsmooth functions satisfying bundary conditions. *Math. Comp.*, 54:483–493, 1990.

[24] K.G. Siebert. An a posteriori error estimator for anisotropic refinement. *Numer. Math.*, 73(3):373–398, 1996.

[25] S.-Y. Yang and J.-L. Liu. A unified analysis of a weighted least squares method for first-order systems. *Appl. Math. Comput.*, 92:9–27, 1998.

Chalmers Finite Element Center Preprints

2001–01 *A simple nonconforming bilinear element for the elasticity problem*
Peter Hansbo and Mats G. Larson

2001–02 *The $\mathcal{LL}^*$ finite element method and multigrid for the magnetostatic problem*
Rickard Bergström, Mats G. Larson, and Klas Samuelsson

2001–03 *The Fokker-Planck operator as an asymptotic limit in anisotropic media*
Mohammad Asadzadeh

2001–04 *A posteriori error estimation of functionals in elliptic problems: experiments*
Mats G. Larson and A. Jonas Niklasson

2001–05 *A note on energy conservation for Hamiltonian systems using continuous time finite elements*
Peter Hansbo

2001–06 *Stationary level set method for modelling sharp interfaces in groundwater flow*
Nahidh Sharif and Nils-Erik Wiberg

2001–07 *Integration methods for the calculation of the magnetostatic field due to coils*
Marzia Fontana

2001–08 *Adaptive finite element computation of 3D magnetostatic problems in potential formulation*
Marzia Fontana

2001–09 *Multi-adaptive galerkin methods for ODEs I: theory & algorithms*
Anders Logg

2001–10 *Multi-adaptive galerkin methods for ODEs II: applications*
Anders Logg

2001–11 *Energy norm a posteriori error estimation for discontinuous Galerkin methods*
Roland Becker, Peter Hansbo, and Mats G. Larson

2001–12 *Analysis of a family of discontinuous Galerkin methods for elliptic problems: the one dimensional case*
Mats G. Larson and A. Jonas Niklasson

2001–13 *Analysis of a nonsymmetric discontinuous Galerkin method for elliptic problems: stability and energy error estimates*
Mats G. Larson and A. Jonas Niklasson

2001–14 *A hybrid method for the wave equation*
Larisa Beilina, Klas Samuelsson and Krister Åhlander

2001–15 *A finite element method for domain decomposition with non-matching grids*
Roland Becker, Peter Hansbo and Rolf Stenberg

2001–16 *Application of stable FEM-FDTD hybrid to scattering problems*
Thomas Rylander and Anders Bondeson

2001–17 *Eddy current computations using adaptive grids and edge elements*
Y. Q. Liu, A. Bondeson, R. Bergström, C. Johnson, M. G. Larson, and K. Samuelsson

2001–18 *Adaptive finite element methods for incompressible fluid flow*
Johan Hoffman and Claes Johnson

2001–19 *Dynamic subgrid modeling for time dependent convection–diffusion–reaction equations with fractal solutions*
Johan Hoffman

2001–20 *Topics in adaptive computational methods for differential equations*
Claes Johnson, Johan Hoffman and Anders Logg

2001–21 *An unfitted finite element method for elliptic interface problems*
Anita Hansbo and Peter Hansbo

2001–22 *A P^2–continuous, P^1–discontinuous finite element method for the Mindlin-Reissner plate model*
Peter Hansbo and Mats G. Larson

2002–01 *Approximation of time derivatives for parabolic equations in Banach space: constant time steps*
Yubin Yan

2002–02 *Approximation of time derivatives for parabolic equations in Banach space: variable time steps*
Yubin Yan

2002–03 *Stability of explicit-implicit hybrid time-stepping schemes for Maxwell's equations*
Thomas Rylander and Anders Bondeson

2002–04 *A computational study of transition to turbulence in shear flow*
Johan Hoffman and Claes Johnson

2002–05 *Adaptive hybrid FEM/FDM methods for inverse scattering problems*
Larisa Beilina

2002–06 *DOLFIN - Dynamic Object oriented Library for FINite element computation*
Johan Hoffman and Anders Logg

2002–07 *Explicit time-stepping for stiff ODEs*
Kenneth Eriksson, Claes Johnson and Anders Logg

2002–08 *Adaptive finite element methods for turbulent flow*
Johan Hoffman

2002–09 *Adaptive multiscale computational modeling of complex incompressible fluid flow*
Johan Hoffman and Claes Johnson

2002–10 *Least-squares finite element method with applications in electromagnetics*
Rickard Bergström

2002–11 *Discontinuous/continuous least-squares finite element methods for Elliptic Problems*
Rickard Bergström and Mats G. Larson

These preprints can be obtained from

`www.phi.chalmers.se/preprints`